1. Marcin DZIADOSZ[3], 2. Mariusz MAZUREK[4], 3. Oleksii HYKA[1], 4. Marcin KOWALSKI[1], 5. Dariusz WÓJCIK[1,2]

R&D Center Netrix S.A. Lublin, Poland (1), WSEI University Lublin, Poland (2), Lublin University of Technology Lublin, Poland (3), Polish Academy of Science Warsaw, Poland (4)
ORCID: 1. 0000-0002-0506-6653, 2. 0000-0002-9646-6897, 3. 0000-0003-2129-5138, 4. 0000-0002-1644-0612, 5. 0000-0002-4200-3432

doi:10.15199/48.2024.04.50

Development and implementation of algorithms for measurement and reconstruction analysis in ultrasound tomography

***Abstract**. The paper presents various machine-learning methods to solve a forward problem for transmission and reflective ultrasound tomography. All described algorithms were trained on a sample from the ultrasound tomography data set. In order to compare the solutions, the image reconstruction quality measures were calculated, such as Mean Absolute Error (MAE), Mean Squared Error (MSE), PSNR (Peak Signal-to-Noise Ratio) and the Structural Similarity Index (SSIM).*

***Streszczenie.** W artykule przedstawiono różne metody uczenia maszynowego do rozwiązania problemu prostego w transmisyjnej i refleksyjnej tomografii ultradźwiękowej. Wszystkie opisane algorytmy trenowano na próbce ze zbioru danych tomografii ultradźwiękowej. W celu porównania rozwiązań obliczono miary jakości rekonstrukcji obrazu, takie jak średni błąd bezwzględny (MAE), błąd średniokwadratowy (MSE), PSNR (szczytowy stosunek sygnału do szumu) oraz wskaźnik podobieństwa strukturalnego SSIM (**Opracowanie i wdrożenie algorytmów do rekonstrukcji pomiarów w tomografii ultradźwiękowej**).*

Keywords: ultrasound tomography, machine learning, forward problem, measurements, reconstruction
Słowa kluczowe: tomografia ultradźwiękowa, uczenie maszynowe, problem prosty, pomiary, rekonstrukcja

Introduction

Tomography is a method of imaging a cross-section of a target based on measurement. In ultrasound tomography (UST) the source of the signal is ultrasound. During the research, two types of ultrasonic tomography were considered – transmission and reflective [1-9].

The forward problem task in tomography aims to reconstruct the measurements. The machine learning models were trained on a data set consisting of input images with some inclusions. The measurements for the ultrasound tomography can be easily visualized [10-16]; however, in order to compare exactly the quality of the models, the image reconstruction assessment measures were calculated, such as Mean Absolute Error (MAE), Mean Squared Error (MSE), PSNR (Peak Signal-to-Noise Ratio) and the Structural Similarity Index Measure (SSIM) [17-20].

Reconstruction Quality Measures

Since assessing the quality of the measurements reconstructions visually might not always be a good indicator, some measures were calculated.
MAE is the Mean Absolute Error. It is expressed by the formula (1):

$$MAE = \frac{1}{n}\sum_{i=1}^{n}|x_i - y_i|, \quad (1)$$

where n is the sample size, x_i denotes the true value and y_i denotes the predicted value. Similarly, MSE (Mean Squared Error) was calculated, which is defined as follows:

$$MSE = \frac{1}{n}\sum_{i=1}^{n}(x_i - y_i)^2, \quad (2)$$

where n is the sample size, x_i is the true value and y_i is the predicted value. The third measure, PSNR (Peak Signal-to-Noise Ratio) is specified as:

$$PSNR = 10 \cdot log_{10}\frac{(max\, x_i)^2}{MSE}, \quad (3)$$

where x_i denotes the true value. The PSNR coefficient depends on the Mean Squared Error. The last considered reconstruction quality indicator, SSIM, is the Structural Similarity Index:

$$SSIM = \frac{(2\mu_x\mu_y + c_1)(2\sigma_{xy} + c_2)}{(\mu_1^2 + \mu_2^2 + c_1)(\sigma_1^2 + \sigma_2^2 + c_2)}, \quad (4)$$

where μ_x, μ_y are the average values of respectively x and y, σ_1^2, σ_2^2 are the variances of respectively x and y, σ_{xy} is the covariance of x and y and finally c_1, c_2 are constant.

During the study described in the article, each of the described measures was calculated for the reconstruction of each image and then averaged.

Methods and Reconstructions

The section presents six machine-learning techniques to solve a forward problem for ultrasonic transmission and reflective tomography. The methods include Elastic Net, Artificial Neural Network (ANN), Convolutional Neural Network, Gated Recurrent Unit Network (GRU), Long Short-Term Memory Network (LSTM) and Transfer Learning based on the RESNET-50 model. All described algorithms were prepared in the RStudio environment based on 5,000 observations from the ultrasound tomography dataset sample. Various tests were carried out to obtain the appropriate hyperparameters for each model.

The first one, Elastic Net comes from the R package called 'glmnet'. To obtain reconstructions of measurements based on the analyzed dataset, 256 Elastic Net models were built.

The independent variables were standardized, and the intercept was included in each model. The 'mixing' parameter (Alpha) was 0.8, while the regularization parameter (Lambda) was set at 0.0000007. The penalty function for the Elastic Net model is defined as follows:

$$(1-\alpha)/2\left|\left|\beta\right|\right|_2^2 + \alpha\left|\left|\beta\right|\right|_1. \quad (5)$$

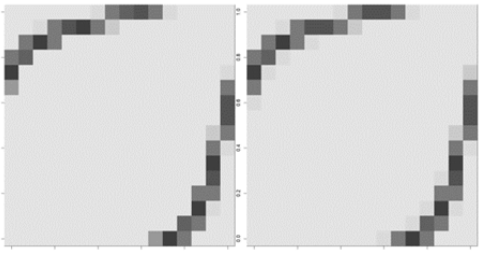

Fig. 1. Exemplary comparison of reference measurements (left) and reconstructed measurements (right) - Elastic Net in Transmission UST

Figure 1 compares original (reference) measurements and the reconstructed ones for the Elastic Net method in ultrasound transmission tomography. Figure 2 compares original (reference) measurements and the reconstructed ones for the Elastic Net method in ultrasound reflective tomography.

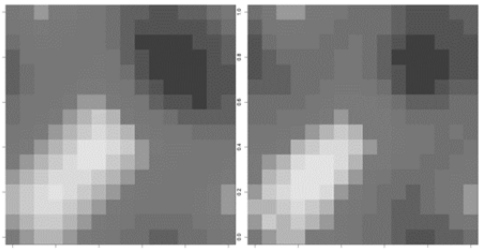

Fig. 2. Exemplary comparison of reference measurements (left) and reconstructed measurements (right) - Elastic Net in Reflective UST

In the next method, an Artificial Neural Network model was built. At the input, there are images with inclusions in a flattened version, while at the output, the entire measurement matrix of ultrasonic tomography is received. The model includes a batch normalization layer, dense layers with the 'relu' activation function and dropout layers. The last dense layer consists of 256 neurons with a linear activation function.

Figure 3 compares original (reference) measurements and the reconstructed ones for the Artificial Neural Network method in ultrasound transmission tomography.

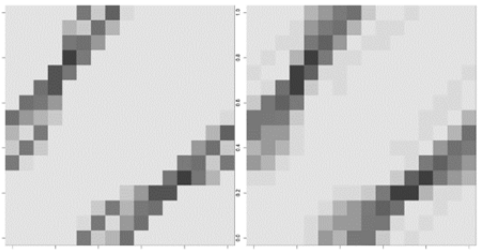

Fig. 3. Exemplary comparison of reference measurements (left) and reconstructed measurements (right) - Artificial Neural Network in Transmission UST

Figure 4 compares original (reference) measurements and the reconstructed ones for the Artificial Neural Network method in ultrasound reflective tomography.

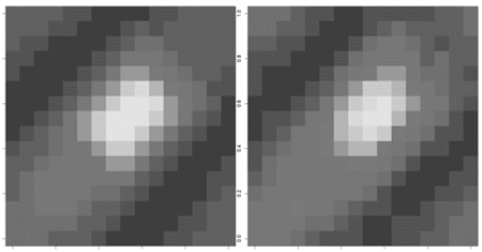

Fig. 4. Exemplary comparison of reference measurements (left) and reconstructed measurements (right) - Artificial Neural Network in Reflective UST

In the third method, a Convolutional Neural Network model was implemented. At the input, there are images with inclusions in a two-dimensional version (not flattened), while at the output, the entire measurement matrix of ultrasonic tomography is returned. In the architecture of the model, there is a batch normalization layer, a two-dimensional convolutional layer containing 128 filters with a 5x5 kernel size and with the 'relu' activation function, a 3x3 max pooling layer, then again a two-dimensional convolutional layer containing 32 filters with a 3x3 kernel size and with the 'relu' activation function and a 2x2 max pooling layer. The last dense layer consists of 256 neurons and has a linear activation function.

Figure 5 compares original (reference) measurements and the reconstructed ones for the Convolutional Neural Network method in ultrasound transmission tomography.

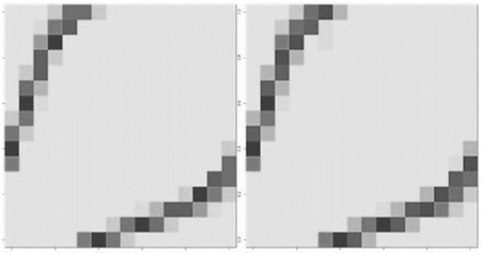

Fig. 5. Exemplary comparison of reference measurements (left) and reconstructed measurements (right) - Convolutional Neural Network in Transmission UST

Figure 6 compares original (reference) measurements and the reconstructed ones for the Convolutional Neural Network method in ultrasound reflective tomography.

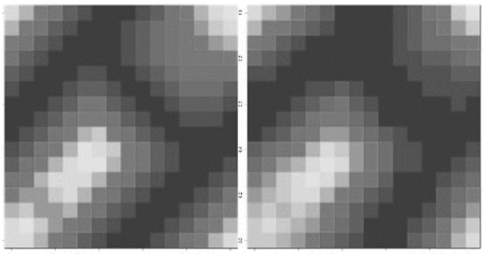

Fig. 6. Exemplary comparison of reference measurements (left) and reconstructed measurements (right) - Convolutional Neural Network in Reflective UST

A Gated Recurrent Unit Network model was built using the following method. At the input, we have images with inclusions again, while at the output, we get the entire measurement matrix of ultrasonic tomography. The model has a batch normalization layer, followed by a Gated Recurrent Unit (GRU) layer with 512 units and with 'dropout' and 'recurrent_dropout' equal to 0.2. The last dense layer has a linear activation function and consists of 256 neurons.

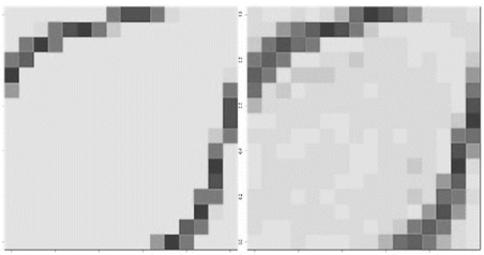

Fig. 7. Exemplary comparison of reference measurements (left) and reconstructed measurements (right) - Gated Recurrent Unit Network in Transmission UST

Figure 7 compares original (reference) measurements and the reconstructed ones for the Gated Recurrent Unit Network method in ultrasound transmission tomography.

Figure 8 compares original (reference) measurements and the reconstructed ones for the Gated Recurrent Unit Network method in ultrasound reflective tomography.

In the fifth method, a Long Short-Term Memory Network model was trained. At the input are images with inclusions, while at the output is the entire ultrasonic tomography measurement matrix. The model has a batch normalization

layer followed by a Long Short-Term Memory (LSTM) layer with 256 units. The last dense layer consists of 256 neurons and has a linear activation function. Figure 9 compares original (reference) measurements and the reconstructed ones for the Long Short-Term Memory Network method in ultrasound transmission tomography.

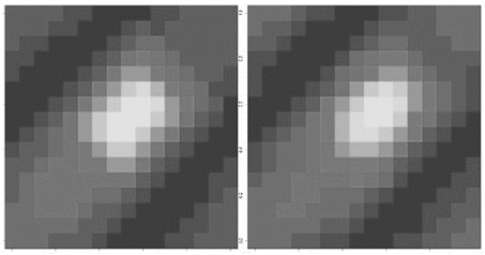

Fig. 8. Exemplary comparison of reference measurements (left) and reconstructed measurements (right) - Gated Recurrent Unit Network in Reflective UST

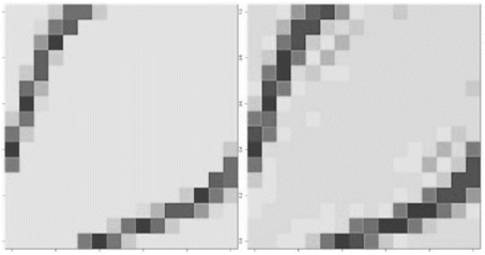

Fig. 9. Exemplary comparison of reference measurements (left) and reconstructed measurements (right) - Long Short-Term Memory Network in Transmission UST

Figure 10 compares original (reference) measurements and the reconstructed ones for the Long Short-Term Memory Network method in ultrasound reflective tomography.

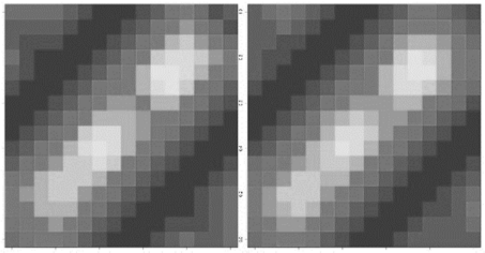

Fig. 10. Exemplary comparison of reference measurements (left) and reconstructed measurements (right) - Long Short-Term Memory Network in Reflective UST

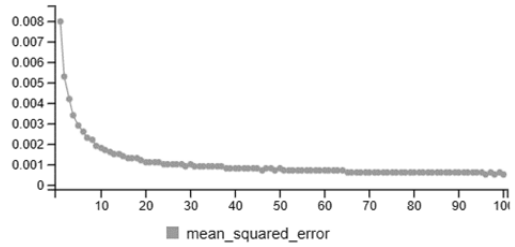

Fig. 11. Transfer learning model training plot for Transmission UST

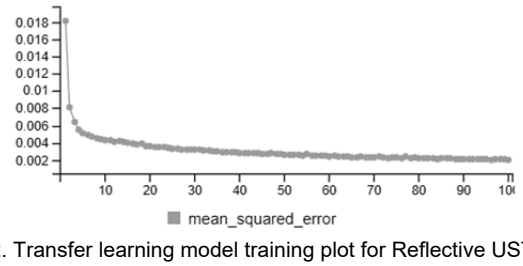

Fig. 12. Transfer learning model training plot for Reflective UST

A transfer learning model based on RESNET-50 was built in the last implemented method. It is a 50-layer convolutional neural network. The data was appropriately prepared for this purpose - images with inclusions were extended by three RGB color channels. The base model is RESNET-50, which consists of 48 convolutional layers, one max pooling layer and one average pooling layer. Base model layers have been excluded from training. Then, a flattened layer and a trainable dense layer with 256 neurons and a linear activation function were applied. The training of the transfer learning model lasted for 100 epochs. Figure 11 and Figure 12 show the MSE loss for both types of ultrasound tomography.

Conclusions and Discussion

In order to accurately compare the quality of the obtained reconstructions of measurements using the described machine learning algorithms, measures such as Mean Absolute Error (MAE), Mean Squared Error (MSE), Peak Signal-to-Noise Ratio (PSNR) and Structural Similarity Index (SSIM) were used. These values were calculated for each reconstructed image and then averaged. Three tables containing the reconstruction quality measures have been created for each type of tomography. Table 1, 2, and 3 refer to the transmission ultrasound tomography. The values in the tables have mostly been rounded.

Table 1. Structural Similarity Index Measure comparison for Transmission UST

Method	SSIM
Elastic Net	0.9999963
CNN	0.9999961
GRU	0.9999861
LSTM	0.9999832
RESNET-50	0.9999760
ANN	0.9999551

It can be concluded that the Structural Similarity Index (SSIM) values are all approximately equal to 1. This fact indicates a high structural similarity of the obtained reconstructions for every technique used. For example, the best value of the SSIM, achieved for the Elastic Net method, is 0.9999963, while the lowest one (for the Artificial Neural Network method) is 0.9999551. The difference between them is just 0.0000412, meaning that the performance of the discussed algorithms in terms of the SSIM indicator is quite similar.

Table 2. Mean Absolute Error and Mean Squared Error comparison for Transmission UST

Method	MAE	MSE
Elastic Net	0.0044	0.00008
CNN	0.0059	0.00012
GRU	0.0140	0.00051
LSTM	0.0143	0.00059
RESNET-50	0.0186	0.00081
ANN	0.0223	0.00170

However, the error values (Mean Absolute Error and Mean Squared Error) are more varied. The Elastic Net and Convolutional Neural Network reconstructions have the smallest MAE and MSE, confirming the predictions' good quality. The MAE for Elastic Net and CNN are respectively 0.0044 and 0.0059. The MSE for Elastic Net and CNN is 0.00008 and 0.00012, accordingly. The two worst-performing algorithms in terms of error value are RESNET-50 (Transfer Learning) and the Artificial Neural Network. The MAE for RESNET-50 and ANN is respectively 0.0186 and 0.0223. The MSE for RESNET-50 and ANN is 0.00081 and 0.00170, respectively. On average, the Gated

Recurrent Unit Network and the Long Short-Term Memory Network are the two algorithms that coped with the measurement reconstruction problem.

Table 3. Peak Signal-to-Noise Ratio comparison for Transmission UST

Method	PSNR
Elastic Net	35.42
CNN	32.02
GRU	24.44
LSTM	24.25
RESNET-50	22.29
ANN	20.26

The Peak Signal-to-Noise Ratio results confirm all the previous conclusions. According to the PSNR measure, the Elastic Net method and the Convolutional Neural Network provide the best forward problem solutions (35.42 and 32.02). The GRU and LSTM methods coped with the reconstruction task similarly at an average level (24.44 and 24.25). The Peak Signal-to-Noise Ratio in the RESNET-50 (Transfer Learning) and ANN cases is the lowest (22.29 and 20.26). Therefore, the Elastic Net and Convolutional Neural Network (CNN) algorithms coped best with the forward problem in the case of ultrasonic transmission tomography.

Authors: *Marcin Dziadosz, M.Sc. Eng., Lublin University of Technology, Nadbystrzycka 38, Lublin, Poland, E-mail: m.dziadosz@pollub.pl; Mariusz Mazurek, Ph.D., Institute of Philosophy and Sociology of the Polish Academy of Science Warsaw, Poland, E-mail: mmazurek@ifispan.edu.pl; Oleksii Hyka, M.Sc. Eng., Research and Development Centre Netrix S.A E-mail: oleksii.hyka@netrix.com.pl; Marcin Kowalski, Ph.D., D.Sc. Eng., WSEI University, Projektowa 4, Lublin, Poland E-mail: marcin.kowalski@wsei.lublin.pl; Dariusz Wójcik, University of Economics and Innovation, Projektowa 4, Lublin, Poland/ Research & Development Centre Netrix S.A. E-mail: dariusz.wojcik@netrix.com.pl*

REFERENCES

[1] Kłosowski G., Rymarczyk T., Kania K., Świć A., Cieplak T., Maintenance of industrial reactors supported by deep learning driven ultrasound tomography, Eksploatacja i Niezawodnosc – Maintenance and Reliability; 22 (2020), No 1, 138–147.

[2] Koulountzios P., Rymarczyk T., Soleimani M., A triple-modality ultrasound computed tomography based on full-waveform data for industrial processes, IEEE Sensors Journal, 21 (2021), No. 18, 20896-20909.

[3] Kak C. Avinash, Slaney Malcolm: Principles of Computerized Tomographic Imaging, The Institute of Electrical and Electronics Engineers, Inc. New York, 1988

[4] Rymarczyk T., Kłosowski G., Kozłowski E., Niderla K., Logistic Regression for Machine Learning in Process Tomography, *Sensors*, 19, (2019), 15, 1-19

[5] Polakowski K., Filipowicz S., Sikora J., Rymarczyk T., Tomography technology application for workflows of gases monitoring in the automotive systems, *Przegląd Elektrotechniczny*, 84 (2008), 227-229

[6] Rymarczyk T., Kłosowski G., Innovative methods of neural reconstruction for tomographic images in maintenance of tank industrial reactors, *Eksploatacja i Niezawodność - Maintenance and Reliability* 21 (2019), nr 2, 261-267

[7] Koulountzios P., Aghajanian S., Rymarczyk T., Koiranen T., Soleimani M., An Ultrasound Tomography Method for Monitoring CO2 Capture Process Involving Stirring and CaCO3 Precipitation, Sensors, 21 (2021), No. 21, 6995.

[8] Mazurek M., Rymarczyk T., Kłosowski G., Maj M., Adamkiewicz P., Tomographic measuring sensors system for analysis and visualization of technological processes, *2020 50th Annual IEEE-IFIP International Conference on Dependable Systems and Networks-Supplemental Volume (DSN-S),* 45-46

[9] Kania K., Rymarczyk T., Maj M., Gołąbek M., Adamkiewicz P., Sikora J., RayIntegration methods for real-time reconstruction using a compact measuring device, *International Interdisciplinary PhD Workshop (IIPhDW)*, (2019), 47-50

[10] Kłosowski G., Rymarczyk T., Niderla K., Rzemieniak M., Dmowski A., Maj M., Comparison of Machine Learning Methods for Image Reconstruction Using the LSTM Classifier in Industrial Electrical Tomography, Energies 2021, 14 (2021), No. 21, 7269.

[11] Rymarczyk T., Kłosowski G., Hoła A., Sikora J., Tchórzewski P., Skowron Ł., Optimising the Use of Machine Learning Algorithms in Electrical Tomography of Building Walls: Pixel Oriented Ensemble Approach, Measurement, 188 (2022), 110581.

[12] Kłosowski G, Rymarczyk T, Niderla K, Kulisz M, Skowron Ł, Soleimani M., Using an LSTM network to monitor industrial reactors using electrical capacitance and impedance tomography – a hybrid approach. Eksploatacja i Niezawodnosc – Maintenance and Reliability, 25 (2023), No. 1, 11.

[13] Fraczyk, A.; Kucharski, J. Surface temperature control of a rotating cylinder heated by moving inductors. Appl. Therm. Eng., 125 (2017), 767–779

[14] Majchrowicz M., Kapusta P., Jackowska-Strumiłło L., Sankowski D., Acceleration of image reconstruction process in the electrical capacitance tomography 3d in heterogeneous, multi-gpu system, Informatyka, Automatyka, Pomiary w Gospodarce i Ochronie Środowiska (IAPGOŚ), 7(2017), No. 1, 37-41

[15] Goetzke-Pala A., Hoła A., Sadowski Ł., A non-destructive method of the evaluation of the moisture in saline brick walls using artificial neural networks. Archives of Civil and Mechanical Engineering, 18 (2018), No. 4, 1729-1742

[16] Styła, M., Adamkiewicz, P., Optimisation of commercial building management processes using user behaviour analysis systems supported by computational intelligence and RTI, Informatyka, Automatyka, Pomiary W Gospodarce I Ochronie Środowiska, 12 (2022), No 1, 28-35.

[17] Gnaś, D., Adamkiewicz, P., Indoor localization system using UWB, Informatyka, Automatyka, Pomiary W Gospodarce I Ochronie Środowiska, 12 (2022), No. 1, 15-19.

[18] Korzeniewska, E., Sekulska-Nalewajko, J., Gocawski, J., Droż Dż, T., Kiebasa, P., Analysis of changes in fruit tissue after the pulsed electric field treatment using optical coherence tomography, EPJ Applied Physics, 91 (2020), No.3, 30902

[19] Sekulska-Nalewajko, J., Gocławski, J., Korzeniewska, E., A method for the assessment of textile pilling tendency using optical coherence tomography, Sensors (Switzerland), 20 (2020), No.13, 1-19, 3687

[20] Pawłowski, S., Plewako, J., Korzeniewska, E., Field modeling the impact of cracks on the electroconductivity of thin-film textronic structures, Electronics (Switzerland), 9 (2020), No.3, 402.